



SAKARYA ÜNİVERSİTESİ

FEN BİLİMLERİ ENSTİTÜSÜ DERGİSİ

Sakarya University Journal of Science
SAUJS

ISSN 1301-4048 e-ISSN 2147-835X Period Bimonthly Founded 1997 Publisher Sakarya University
<http://www.saujs.sakarya.edu.tr/>

Title: Some Electrical and Photoelectrical Properties of Conducting Polymer Graphene Composite /n-Silicon Heterojunction Diode

Authors: Elif DAŞ

Received: 2022-06-14 00:00:00

Accepted: 2022-08-31 00:00:00

Article Type: Research Article

Volume: 26

Issue: 5

Month: October

Year: 2022

Pages: 2000-2009

How to cite

Elif DAŞ; (2022), Some Electrical and Photoelectrical Properties of Conducting Polymer Graphene Composite /n-Silicon Heterojunction Diode. Sakarya University Journal of Science, 26(5), 2000-2009, DOI: 10.16984/saufenbilder.1129742

Access link

<http://www.saujs.sakarya.edu.tr/en/pub/issue/73051/1129742>

New submission to SAUJS

<http://dergipark.gov.tr/journal/1115/submission/start>

Some Electrical and Photoelectrical Properties of Conducting Polymer Graphene Composite /n-Silicon Heterojunction Diode

Elif DAŞ*¹

Abstract

In this study, polythiophene-graphene (PTh-G) composite thin film was prepared on the n-type silicon (n-Si) semiconductor wafer by the spin coating method. Subsequently, the current-voltage (I-V) measurements were made on the fabricated Au/PTh-G/n-Si/Al device to ascertain the impact of the PTh-G interfacial layer on the device performance. The main device parameters such as ideality factor (n), barrier height (Φ_b), series resistance (R_s) were calculated by using the thermionic emission (TE) and Norde functions, and then, the obtained results were discussed in detail. Additionally, the capacitance-voltage (C-V) characteristic of the device was examined as a function of the frequency, and the device parameters such as diffusion potential (V_d), Fermi energy level (E_f), carrier concentration (N_d), Φ_b were determined. Finally, the light intensity-dependent I-V measurements were taken to obtain information about the photoelectrical characteristics of the fabricated device. The obtained results have shown that the prepared composite material has a good potential to be used in optoelectronic applications such as photodiode, and photodetector.

Keywords: Polythiophene, graphene, composite material, photoresponse, photosensitivity

1. INTRODUCTION

The metal-semiconductor (MS) Schottky barrier diode (SBD), formed by putting a metal in contact with a semiconductor, is the simplest known form of the electronic rectifier [1-3]. Despite its simple structure, it offers tremendous performance and is used in many different applications. In an SBD, the electrical properties of the device are mainly related to the interface and depletion region of the junction. So, if an interlayer material is positioned

between the semiconductor and the metal, the performance of the device will depend on the physical characteristics of the material [4-6]. Thus, it is possible to fabricate semiconductor devices with higher electrical performance. Many researchers have been researching on using conducting polymer-based materials as interface materials to alter the electrical characteristics of MS junctions in recent years [7, 8].

Conducting polymers and/or their composites have the potential to dissolve in different solvents,

* Corresponding author: das.elif@gmail.com

¹ Atatürk University

ORCID: <https://orcid.org/0000-0002-3149-6016>

which allows them to be easily used in device fabrication via spin coating and drop-casting. Up to now, a wide range of conducting polymers and their derivatives have been developed, such as poly (1,4-phenylenevinylene) (PPV), poly(p-phenylene) (PPP), polyfluorene (PF), and polythiophene (PTh) [8, 9]. Among these conducting polymers, polythiophene (PTh) has been much interested material due to its good chemical and thermal stability as well as excellent electronic and optical properties [10, 11]. Additionally, many composites of PTh have been reported for different applications [9, 12]. The obtained results have shown that composite materials possess properties that may not be achieved by either component separately. Also, these reports have shown that there are many factors affect the PTh composite properties, like synthesis methods, types of fillers, fillers morphology, polymer matrix, etc.

In the last few years, the fantastic properties of carbon-based materials make them very promising and favorable as fillers for production of a new class of polymeric heterostructures. For example, Wang et al. [13] prepared ordered PTh/fullerene composite core-shell nanorod arrays by using melt-assisted wetting of porous alumina templates. Experimental results showed that the synthesized material has promising potential in solar cells. Also, Karim et al. [14] prepared PTh/single-wall carbon nanotube composites using a polymerization method. The obtained results showed that the composite material was better in terms of thermal and electrical conductivity compared to pure PTh. In another study, Bachhac and Patil [15] synthesized PTh-coated multiwalled carbon nanotube (MWCNT) composites by simple, cost-effective, in-situ oxidative polymerization method. They highlight that synergistic effects of the PTh-coated MWCNTs improve the gas sensing properties. In a nutshell, combining conducting polymers with carbon-based materials allows engineers to create flexible composites with favorable electrical, optical, or mechanical properties. In the light of this information, within the scope of the presented study, the synthesis of PTh-graphene (PTh-G) composite material and its analysis in terms of electrical and photoelectrical

properties at the metal-semiconductor interface are discussed. When the studies in the literature are analyzed, this study is the first research study conducted for the stated purpose. In this sense, I believe that the presented study will make significant contributions to the literature and optoelectronic technology.

2. MATERIALS AND METHODS

2.1. Materials

Thiophene (Sigma-Aldrich), Graphene nanoplatelet (Nanografi, surface area: $320 \text{ m}^2\text{g}^{-1}$), chloroform, anhydrous ferric chloride (FeCl_3), acetone and methanol (Sigma-Aldrich) were used as obtained. Additionally, in the SBDs fabrication process, n-type Si wafer was preferred. A well-known cleaning procedure was used to clean the Si wafers, as specified in ref [16].

2.2. Preparation of PTh-G Composite Materials

Composite materials synthesis were carried out according to a literature method developed by Melo et al. [17] with some modification. In this method, in-situ chemical oxidative polymerization technique was used for the synthesis of composite materials. Briefly, 0.03 g of thiophene monomer was added to chloroform and thoroughly mixed. Then, 0.1 g of graphene was added to the prepared suspension and mixed for a while. On the other hand, 3 g of oxidizing agent FeCl_3 was dispersed in a different beaker with a chloroform solution until it formed a homogeneous suspension. Subsequently, the FeCl_3 suspension was added drop by drop to the thiophene-graphene suspension and stirred for one day at room temperature. After that the PTh-G composite was filtered and attentively washed many times by methanol, water, and acetone, respectively. Finally, the resultant composite material was dried in a vacuum oven.

2.3. Fabrication of Au/PTh-G/n-Si/Al SBD

In this stage, firstly, the aluminum (Al) metal coating process was carried out to obtain ohmic contact onto the unpolished surface of the Si wafer under 10^{-6} torr pressure. Then, the n-Si/Al

structure was maintained at 450 °C for 5 minutes to enhance the ohmic contact's quality. Next stage, the composite material was dispersed in ethanol, then spin-coated onto Si substrate at the rotation of 1000 rpm for one minute, and air-dried overnight at room temperature. Gold (Au) dots were made on the surface of the composite thin film by using thermal evaporation system through a shadow mask. As a result, the fabrication of the Au/PTh-G/n-Si/Al device was completed. The schematic representation of the obtained device structure is given in Figure 1. In addition, reference device (Au/n-Si/Al) fabrication was also performed in order to observe the effect of the composite interfacial material on the junction parameters.

2.4. I-V and C-V Measurements

The I-V measurements of the device were carried out under darkness and illumination conditions using Keithley source-meter. Additionally, the impedance analyzer system ((HP 4192A LF Model) was used to determine the C-V behaviors at various frequencies. The measurements were performed at ambient conditions. More information on measurement systems can be found in previous studies [5,6].

3. RESULTS AND DISCUSSION

3.1. I-V Results of the Fabricated Devices

The forward and reverse biased log (I)-V characteristics of the PTh-G/n-Si and reference diode are shown at dark ambient in Figure 2. According to the literature reports, the non-linear current-voltage characteristics of the metal/polymer junction could be owing to the thermionic emission (TE), space charge limited conduction (SCLC), or Poole-Frenkel emission [18]. The current through a Schottky barrier diode under a forward bias voltage is formulated by the eq. (1)

$$I = I_0 \left[\exp\left(\frac{qV}{nkT}\right) - 1 \right] \quad (1)$$

In eq. (1), electronic charge, voltage, ideality factor, Boltzmann constant, temperature, and saturation current are represented by the terms q , V , n , k , T and I_0 , respectively. I_0 , namely, the

reverse saturation current can be calculated using the equation (2) [19].

$$I_0 = AA^*T^2 \exp(-q\Phi_b/kT) \quad (2)$$

herein, the A is the diode area, A^* is the effective Richardson constant, and Φ_b is Schottky barrier height. If we rearrange the eqs. (1) and (2), the value of n and Φ_b can be calculated from the following equations [20].

$$n = \frac{q}{kT} \left(\frac{dV}{d \ln I} \right) \quad (3)$$

and

$$\Phi_b = \frac{kT}{q} \ln \left(\frac{AA^*T^2}{I_0} \right) \quad (4)$$

In the heterojunction devices, the current transport mechanism is generally analyzed using the TE model. According to the TE model, the n and the Φ_b values of the prepared devices were calculated and the results were tabulated in Table 1. It is clearly seen that the n value of the device obtained with the conductive polymer composite material is lower than the reference diode. The value of n generally expresses the dependence of the diode current on the applied potential and gives information about the quality of the fabricated device. For an ideal SBD, the value of n is equal to one, but, in application, n always exceed unity. In the present study, the value of n is small and closer to unity for the PTh-G/n-Si device. Additionally, the leakage current of the PTh-G/n-Si device is lower than the reference diode as seen in Figure 2. Therefore, it can be said that the electrical properties of the reference diode were improved after the insertion of the PTh-G composite layer between Au and n-Si wafer. On the other hand, Φ_b is a main parameter to specify the attitude of the depletion region in the SBD.

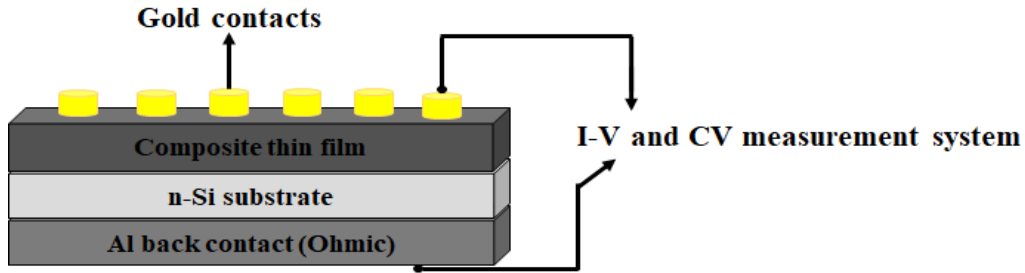


Figure 1 A schematic representation of Au/PTh-G/n-Si/Al SBD

The Φ_b value of the PTh-G/n-Si diode was found as 0.78 eV, which is higher than that of the reference diode (0.74 eV). This situation can be attributed to the presence of the PTh-G composite interlayer. Since the composite thin film separates the metal from the semiconductor material, thereby, an increase in the Φ_b of MS junction is observed.

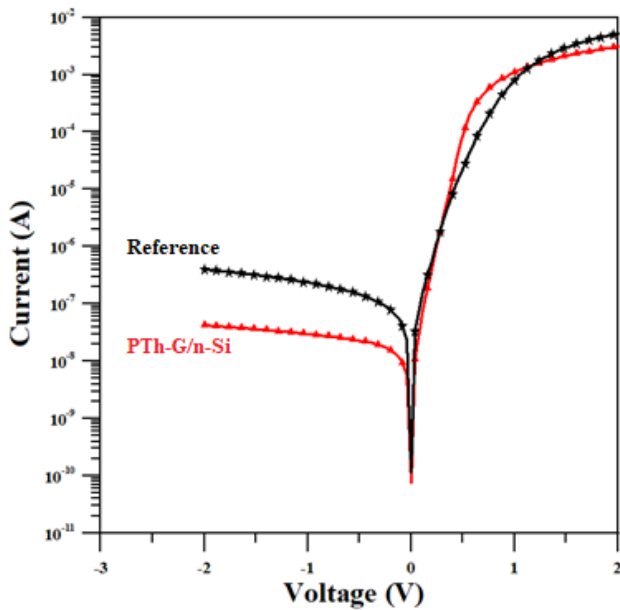


Figure 2 The log (I)-V plots of the PTh-G/n-Si and reference diode at room temperature

In order to get further insight into the electrical properties of the prepared device, determining the value of the series resistance (R_s) is also quite important. The value of R_s can be easily calculated by the Norde method which is described as [21]:

$$F(V) = \frac{V}{\gamma} - \frac{kT}{q} \ln \left(\frac{I(V)}{AA^*T^2} \right) \quad (5)$$

here, γ is the first integer greater than n . The value of R_s is determined using the following equation:

$$R_s = \frac{kT(\gamma-n)}{qI} \quad (6)$$

here the n value obtained from the $\ln(I)$ -V plot is used. Moreover, the value of the Φ_b can be computed using this method. The Φ_b is given as

$$\Phi_b = F(V_{min}) + \frac{V_{min}}{\gamma} - \frac{kT}{q} \quad (7)$$

The lowest level of $F(V)$ is $F(V_{min})$, and V_{min} is the corresponding voltage value. Figure 3 shows Norde's function against the potential for the PTh-G/n-Si heterojunction device. Based on equations (6) and (7), the Φ_b and R_s values of the devices were calculated and summarized in Table 1. According to acquired the results, the values of Φ_b are in good agreement with those obtained from I-V characteristics.

3.2. C-V Results of the PTh-G/n-Si SBD

The C-V measurement provides important information about the interfacial properties of the diode. For this purpose, the C-V measurements of the PTh-G/n-Si heterojunction device were carried out at room temperature, with a frequency range of 100-1000 kHz. The obtained C-V characteristics for the PTh-G/n-Si device are shown in Figure 4, and the relationship for C^{-2} -V characteristics are shown in Figure 5. In Figure 4, the capacitance increases with the applied voltage in the forward bias region up to a point where it

Table 1 Main device parameters of the fabricated devices

Device (dark ambient)	I-V		Norde	
	n	Φ_b (eV)	Φ_b (eV)	R_s (Ω)
Au/n-Si/Al	2.67	0.74	0.74	2762
Au/PTh-G/n-Si/Al	1.84	0.78	0.77	3479

reaches a maximum value. Also, the value of the capacitance at the peak tends to decrease with increasing frequency. The increase in peak value of the capacitance occurs because the interface states at lower frequencies can follow the alternative current (AC) signal and yield an excess capacitance which depends on the frequency [22]. However, in the high frequency limit, the contribution of the interface states which can follow the AC signal, to the total capacitance is negligibly small. Hence, the capacitance peak tends to decrease as frequency increases.

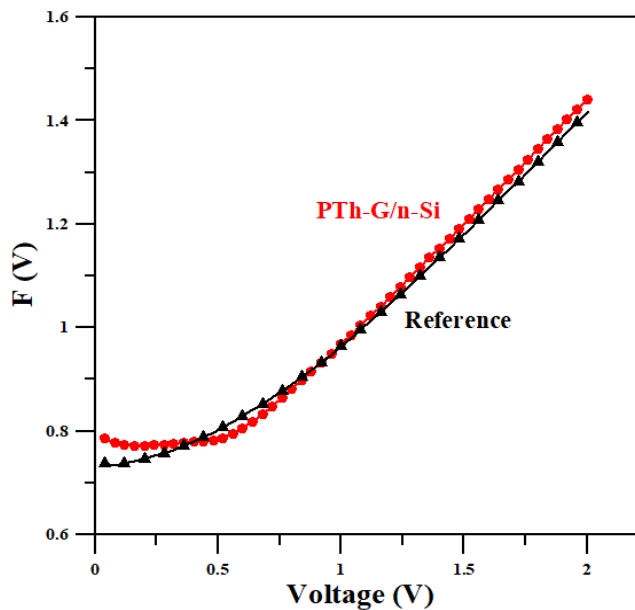


Figure 3 The F(V)-V plots of the PTh-G/n-Si and reference device

Additionally, in Figure 5, C^{-2} -V plot of the PTh-G/n-Si diode exhibits a linear behavior in the negative voltage range for all frequency values, and at this region, the equation for the connection between C^{-2} and V_d can be given as eq.(8) [22, 23].

$$C^{-2} = \frac{2(V_d+V)}{q\epsilon_s N_d A^2} \quad (8)$$

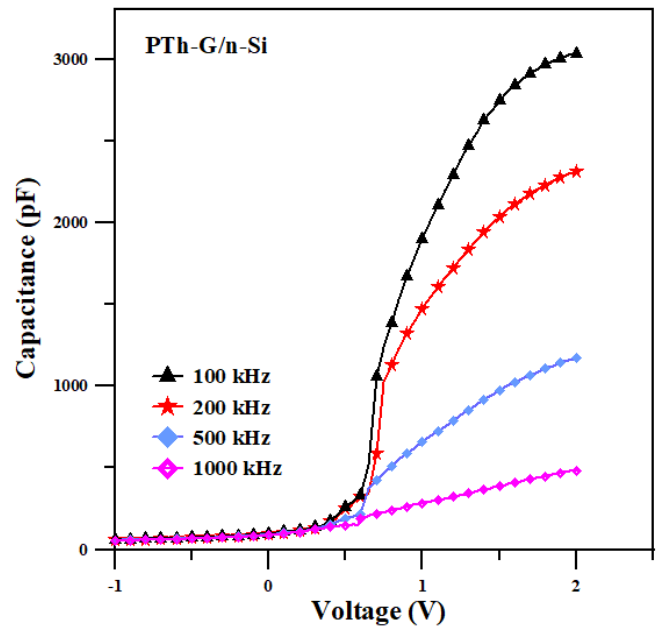


Figure 4 The C-V curves of the PTh-G/n-Si SBD for different frequencies

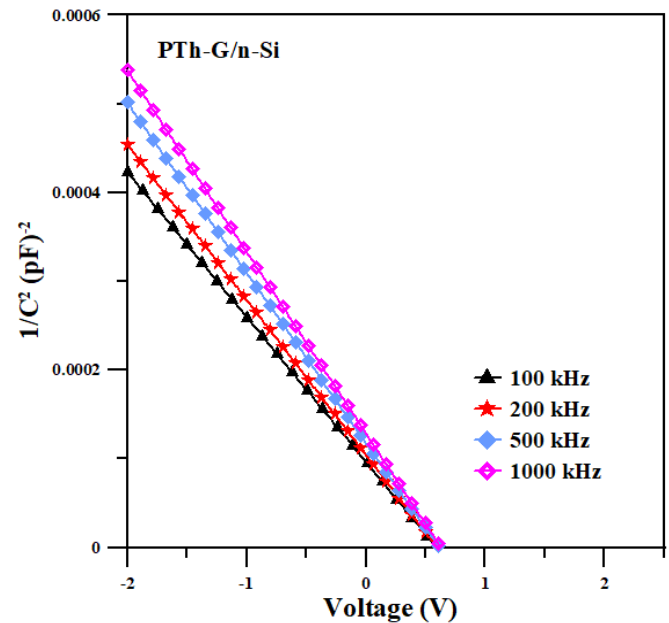


Figure 5 The C^{-2} -V curves of the PTh-G/n-Si SBD for different frequencies

Table 2 The device parameters obtained from C^{-2} -V plot for characteristics of the Au/PTh-G/n-Si/Al SBD between 100 and 1000 kHz at the room temperature

Frequency (kHz)	V_d (V)	N_d (cm ⁻³)	E_f (eV)	Φ_b (eV)
1000	0.651	$9.68 \cdot 10^{14}$	0.265	0.60
500	0.628	$1.02 \cdot 10^{15}$	0.264	0.59
200	0.605	$1.11 \cdot 10^{15}$	0.262	0.57
100	0.590	$1.18 \cdot 10^{15}$	0.260	0.56

herein, V_d is the diffusion potential at zero bias which is determined from the extrapolation of the linear C^{-2} -V plot to V axis. Also, ϵ_s is the dielectric constant of semiconductor, A is the effective area of the diode and N_d is the concentration of ionized donors.

In order to determine device parameters of the PTh-G/n-Si diode, the C-V curves were used, and the obtained results were given in Table 2. According to the results, it can be said that the parameters show a weak frequency dependency in the applied frequency range. The similar results for these parameters can be found in the literature reports [24, 25].

3.3. Photocurrent and Responsivity Measurements

Figure 6 show the effect of illumination on the PTh-G/n-Si device. It is seen that the diode current does not change in the forward bias region under white light illumination, on the other hand, it increases with increasing light intensity in the reverse bias region. Such behavior implies that the device has a photodiode characteristic. Furthermore, at zero bias, the short circuit current (I_{sc}) is sensitive to the intensity of the light. So, it can be said that self-powered light detection can be achieved with the PTh-G/n-Si SBD [26].

In the literature, the photoresponsivity (R) and photosensitivity (S) behavior of the SBDs are usually investigated for photoconductivity measurements [26-29]. In this sense, we can say that the responsivity is a way to show the photoconductivity or the light-induced current of a material. The value of R is defined as the ratio of electrical output to its optical input in Amperes/Watt (AW^{-1}), as shown in equation (9).

$$R = \frac{J_{ph}}{P_{in}} \quad (9)$$

where, J_{ph} is the photocurrent density, P_{in} is the incident light power. On the other hand, the photosensitivity is simply the ON/OFF ratio for current output in the light compared to that in the dark, as shown in equation (10).

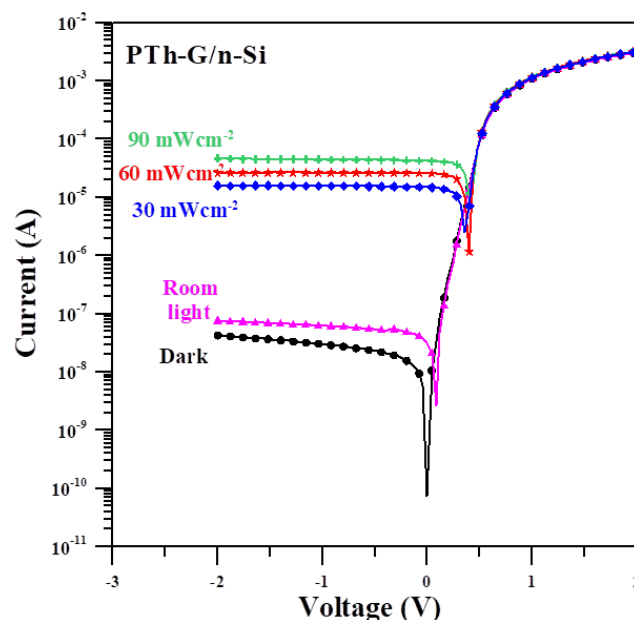


Figure 6 The I-V plots of the PTh-G/n-Si device under dark and different light illuminations

$$S = \frac{I_{ph}}{I_{dark}} \quad (10)$$

In the light of this information, the R and S values of the PTh-G/n-Si device were calculated at different voltages for various light intensities and the obtained results were tabulated in Table 3. It is seen that the R and S values of the device vary depending on the incident light power. Additionally, open-circuit voltage (V_{oc}) and (I_{sc})

Table 3 Photodiode parameters of the PTh-G/n-Si SBD at various light intensities

Light Intensity (mWcm ⁻²)	I _{sc} (μA)	V _{oc} (V)	Photosensitivity (S)		Photoresponsivity (R) (AW ⁻¹)	
			(@-0.5 V)	(@-1 V)	(@-0.5 V)	(@-1 V)
30	13.2	0.37	676.4	517.1	6.5*10 ⁻²	6.6*10 ⁻²
60	23.8	0.40	1159.4	875.6	5.6*10 ⁻²	5.6*10 ⁻²
90	36.8	0.41	1936.1	1480.9	6.2*10 ⁻²	6.3*10 ⁻²

Table 4 Photovoltaic parameters of the PTh-G/n-Si and reported polymer/Si based junctions

Device configuration	Light Intensity (mWcm ⁻²)	I _{sc} (μA)	V _{oc} (V)	References
PTh-G/n-Si	90	36.8	0.41	present work
CU:rGO/n-Si	10	0.48	0.22	[30]
	150	12.18	0.37	
bisTPAT/n-Si	100	15	0.40	[31]
PVA(Co-doped)/n-Si	100	19.30	0.28	[32]
PVA (Bi-doped)/n-Si	250	88.53	0.22	[33]
PVA (Ni-doped)/n-Si	100	33.2	0.42	[34]
Pentacene/n-Si	100	~7	~0.15	[35]
Sunset Yellow/n-Si	40	25.45	~0.15	[36]
	100	91.84	~0.18	
Eosin y/n-Si	100	10	0.02	[37]
Eosin y/p-Si	100	9	0.10	

values of the PTh-G/n-Si device were also given in Table 3. The results demonstrated that when light intensity increased, the photovoltaic parameters improved. Furthermore, the photovoltaic parameters were compared with the relevant literature reports in the Table 4. The obtained values suggest that the PTh-G/n-Si device can be operated as a heterojunction photodiode.

4. CONCLUSION

In recent years, extensive research has been carried out on conductive polymer carbon-based composite materials for various applications due to their extraordinary properties. In the presented study, the performance of PTh-G composite material as an interface layer in the Au/PTh-G/n-Si/Al SBD structure was evaluated for the first time in the literature. For this purpose, firstly,

PTh-G composite material synthesis was made by using the in-situ chemical oxidative polymerization method, and then device fabrication was carried out. The I-V characteristics of the prepared device were measured under dark and illuminated conditions (30-90 mWcm⁻²) to provide information about important device parameters such as n, Φ_b, R_s, R, and S. The obtained results show that the device is highly sensitive to light and exhibits a self-powering feature under illumination. Additionally, C-V measurements show that the fabricated device has capacitance feature and this capacity change as a function of the frequency. So, based on the obtained results, it can be said that the fabricated Au/PTh-G/n-Si/Al SBD can be used in optoelectronic applications.

Funding

The author has not received any financial support for the research, authorship or publication of this study.

Acknowledgements

I would like to thank the NANOGRAFI Company (Turkey) for supplying graphene in this study. Also, I would like to express my special thanks to Mr. Zafar Alam Queraishi for his valuable time and useful suggestions.

The Declaration of Conflict of Interest/ Common Interest

No conflict of interest or common interest has been declared by the author.

Authors' Contribution

ED: This paper is a single-author study. Everything was done by the author.

The Declaration of Ethics Committee Approval

The author declares that this document does not require an ethics committee approval or any special permission.

The Declaration of Research and Publication Ethics

The author of the paper declares that they comply with the scientific, ethical and quotation rules of SAUJS in all processes of the paper and that they do not make any falsification on the data collected. In addition, they declare that Sakarya University Journal of Science and its editorial board have no responsibility for any ethical violations that may be encountered, and that this study has not been evaluated in any academic publication environment other than Sakarya University Journal of Science.

REFERENCES

- [1] S. M. Sze, "Physics of Semiconductor Devices," 2nd ed. Wiley, New York, 1981.
- [2] E. H. Rhoderick, R. H. Williams, Metal-Semiconductor Contacts, 2nd ed., Clarendon Press, Oxford, 1988.
- [3] R. T. Tung, "Recent advances in Schottky barrier concepts," *Materials Science and Engineering R*, vol. 35, pp. 1-138, 2001.
- [4] Z. Çaldıran, "Modification of Schottky barrier height using an inorganic compound interface layer for various contact metals in the metal/p-Si device structure," *Journal of Alloy and Compound*, vol. 865, pp. 158856, 2021.
- [5] E. Daş, "Electrical and photoelectrical properties of Schottky diode construction with three-dimensional (3D) graphene aerogel interlayer," *Optical Materials*, vol. 121, pp. 111633, 2021.
- [6] E. Daş, "Green synthesis of reduced graphene oxide and device fabrication for optoelectronic applications," *Erzincan University Journal of Science and Technology*, vol. 14, pp. 524-541, 2021.
- [7] S. Mahato, "Composition analysis of two different PEDOT:PSS commercial products used as an interface layer in Au/n-Si Schottky diode," *RSC Advances*, vol. 7, pp. 47125, 2017.
- [8] S. Ying, Z. Ma, Z. Zhou, R. Tao, K. Yan, M. Xin, Y. Li, L. Pan, A. Y. Shi, "Device based on polymer Schottky junctions and their applications: A review," *IEEE Access*, vol. 8, pp. 189646-189660, 2020.
- [9] F. Vatansever, J. Hacıoğlu, U. Akbulut, L. Toppare, "A conducting composite of polythiophene: synthesis and characterization," *Polymer International*, vol. 41, pp. 237-244, 1996.
- [10] K. R. Nemade and S. A. Waghuley, "Synthesis, characterization and thermal properties of polythiophene composites," *Asian Journal of Chemistry*, vol. 24, pp. 5947-5948, 2012.
- [11] S. Sivrikaya, A. Dalmaz, S. Durmuş, "Synthesis of nano poly(2-thiophenecarboxaldehyde) and characterization of structure," *Sakarya*

- University Journal of Science, vol. 22, pp. 1571-1575, 2018.
- [12] C. Zanardi, F. Terzi, R. Seeber, "Polythiophenes and polythiophene-based composites in amperometric sensing," *Analytical and Bioanalytical Chemistry*, vol. 405, pp. 509-531, 2013.
- [13] H. S. Wang, L. H. Lin, S. Y. Chen, Y. L. Wang, K. H. Wei, "Ordered polythiophene/fullerene composite core-shell nanorod arrays for solar cell applications," *Nanotechnology*, vol. 20, pp. 075201, 2009.
- [14] M. R. Karim, C. J. Lee, M. S. Lee, "Synthesis and characterization of conducting polythiophene/carbon nanotubes composites," *Journal of Polymer Science (Part A) Polymer Chemistry*, vol. 44, pp. 5283-5290, 2006.
- [15] S. G. Bachhav and D. R. Patil, "Preparation and Characterization of Multiwalled Carbon Nanotubes-Polythiophene Nanocomposites and its Gas Sensitivity Study at Room Temperature," *Journal of Nanostructures*, vol. 7, pp. 247-257, 2017.
- [16] Z. Çaldıran, "Fabrication of Schottky barrier diodes with the lithium fluoride interface layer and electrical characterization in a wide temperature range," *Journal of Alloy and Compounds*, vol. 816, pp. 152601, 2020.
- [17] J. P. Melo, E. N. Schulz, C. M. Verdejo, S. L. Horswell, M. B. Camarada, "Synthesis and Characterization of Graphene/Polythiophene (GR/PT) Nanocomposites: Evaluation as High-Performance Supercapacitor Electrodes," *International Journal of Electrochemical Science*, vol. 12, pp. 2933-2948, 2017.
- [18] R. Singh, D. N. Srivastava, R. A. Singh, "Schottky diodes based on some semiconducting polymers," *Synthetic Metals*, vol. 121, pp. 1439-1440, 2001.
- [19] R. K. Gupta and R. A. Singh, "Schottky diode based on composite organic semiconductors," *Material Science in Semiconductor Processing*, vol. 7, pp. 83-87, 2004.
- [20] R. K. Gupta, K. Ghosh, P. K. Kahol, "Fabrication and electrical characterization of Au/p-Si/STO/Au contact," *Current Applied Physics*, vol. 9, pp. 933-936, 2009.
- [21] H. Norde, "A modified forward I-V plot for Schottky diodes with high series resistance," *Journal of Applied Physics*, vol. 50, pp. 5052-5053, 1979.
- [22] S. A. Yerişkin, M. Balbaş, İ. Orak, "Frequency dependent electrical characteristics and origin of anomalous capacitance-voltage (C-V) peak in Au/(graphene-doped PVA)/n-Si capacitors," *Journal of Materials Science: Materials in Electronics*, vol. 28, pp. 7819-7826, 2017.
- [23] A. Chelkowski, "Dielektrik Physics," Elsevier, Amsterdam, pp. 97-105, 1980.
- [24] S. Demirezen, İ. Orak, Y. Azizian-Kalandaragh, Ş. Altındal, "Series resistance and interface states effects on the C-V and G/w-V characteristics in Au/(Co₃O₄-doped PVA)/n-Si structure at room temperature," *Journal of Materials Science: Materials in Electronics*, vol. 28, pp. 1296-12976, 2017.
- [25] A. Nikravan, Y. Badalı, Ş. Altındal, I. Uslu, İ. Orak, "On the Frequency and Voltage-Dependent Profiles of the Surface States and Series Resistance of Au/ZnO/n-Si Structures in a Wide Range of Frequency and Voltage," *Journal of Electronic Materials*, vol. 46, pp. 5728-5736, 2017.
- [26] K. Chandra Sekhar Reddy, P. Sahatiya, I. Santos-Saucesa, O. Cortazar, R. Ramirez-Bon, "One-step fabrication of 1D p-NiO nanowire/n-Si heterojunction: Development of self-powered ultraviolet

- photodetector,” *Applied Surface Science*, vol. 513, pp. 145804, 2020.
- [27] E. Daş, U. Incekara, Ş. Aydoğan, “A comparative study on electrical characteristics of Ni/n-Si and Ni/n-Pi Schottky diodes with Pinus Sylvestris Resin interfacial layer in dark and under illumination at room temperature,” *Optical Materials*, vol. 119, pp. 111380, 2021.
- [28] Ö. Sevgili and İ. Orak, “The investigation of current condition mechanism of Al/Y₂O₃/p-Si Schottky barrier diodes in wide range temperature and illuminate,” *Microelectronics Reliability*, vol. 117, pp. 114040, 2021.
- [29] A. Koçyiğit, A. Sarılmaz, T. Öztürk, F. Özel, M.Yıldırım, “A Au/CuNiCoS₄/p-Si photodiode: electrical and morphological characterization,” *Beilstein Journal of Nanotechnology*, vol. 12, pp. 984-994, 2021.
- [30] H. O. Doğan, Z. Orhan, F. Yıldırım, S. Aydoğan, “Self-powered photosensor based on curcumin:reduced graphene oxide (Cu:rGO)/n-Si heterojunction in visible and UV regions,” *Journal of Alloys and Compounds*, vol. 915, pp. 165428, 2022.
- [31] M. Erdogan, Z. Orhan, E. Daş, “Synthesis of electron-rich thiophene triphenylamine based organic materials for photodiode applications,” *Optical Materials*, vol. 128, pp. 112446, 2022.
- [32] M. Gökçen, T. Tunç, Ş. Altındal, İ. Uslu, “Electrical and photocurrent characteristics of Au/PVA(Co-doped)/n-Si photoconductive diodes,” *Materials Science and Engineering B*, vol. 177, pp. 416-420, 2012.
- [33] S. Demirezen, Ş. Altındal, İ.Uslu, “Two diodes model and illumination effect on the forward and reverse bias I-V and C-V characteristic of Au/PVA (Bi-doped)/n-Si photodiode at room temperature,” *Current Applied Physics*, vol. 13, pp. 53-59, 2013.
- [34] T. Tunç, M. Gökçen, “Preparation and electrical characterization of Au/n-Si (110) structure with PVA-nickel acetate composite film interfacial layer,” *Journal of Composite Materials*, vol. 46, pp. 2843-2850, 2012.
- [35] H. Kacus, M.Yılmaz, A. Koçyiğit, U. Incekara, Ş. Aydoğan, “Optoelectronic properties of Co/pentacene/Si MIS heterojunction photodiode,” *Physica B: Condensed Matter*, vol. 597, pp. 412408, 2020.
- [36] A. G. Imer, E. Kaya, A. Dere, A. G. Al-Sehemi, A. A. Al-Ghamdi, A. Karabulut, F. Yakuphanoglu, “Illumination impact on the electrical characteristics of Au/Sunset Yellow/n-Si/Au hybrid Schottky diode,” *Journal of Materials Science:Materials in Electronics*, vol. 31, pp. 14665-14673, 2020.
- [37] M.Yılmaz, A. Koçyiğit, S. Aydoğan, U. Incekara, Y. Şahin, H. Kacus, “Influence of illumination intensity on electrical characteristics of Eosin y dye based hybrid photodiode:comparative study,” *Applied Physics A*, vol. 126, pp. 781, 2020.